JOURNAL OF NANO- AND ELECTRONIC PHYSICS
Vol. **18** No 2, 02038(5pp) (2026)

ЖУРНАЛ НАНО- ТА ЕЛЕКТРОННОЇ ФІЗИКИ
Том **18** № 2, 02038(5cc) (2026)

OPEN ACCESS

REGULAR ARTICLE

Properties of Sn-doped ZnO Thin Films Elaborated by Solar Spray Pyrolysis for Photovoltaic Applications

Abdelbaki Nid[1,2,3], Lilia Zighed[1,2,3], Yacine Aoun[4], Said Benramache[5,*]

[1] *Mechanical Department, Faculty of Technology, University of Skikda, Skikda 21000, Algeria*
[2] *LGMM Laboratory, Faculty of Technology, University of Skikda, Skikda 21000, Algeria*
[3] *LGCES Laboratory, Faculty of Technology, University of Skikda, Skikda 21000, Algeria*
[4] *Mechanical Department, Faculty of Technology, University of El-Oued, El-Oued 39000, Algeria*
[5] *Laboratoire des Matériaux, des Énergies et de l'Environnement, University of Biskra 07000, Algeria*

(Received 12 September 2025; revised manuscript received 24 April 2026; published online 29 April 2026)

In this experimental work, pure ZnO and tin-doped ZnO (ZnO:Sn) thin films were successfully deposited onto glass substrates using the solar spray pyrolysis technique. The substrates were heated to approximately 400 °C using a solar furnace. The structural, optical, and electrical properties of the prepared Sn-doped ZnO films were investigated at different tin doping concentrations (0, 1, 3, 5, and 7 at. %). X-ray diffraction (XRD) analysis revealed that all the films exhibit a polycrystalline hexagonal wurtzite structure with a preferred orientation along the (002) plane. UV-Vis spectroscopic measurements showed that all films possess good optical transparency, with a high transmittance of about 90 % for the film doped with 3 at. % Sn. The optical band gap was found to increase from 3.23 to 3.34 eV with increasing tin content. Electrical measurements indicated that films with tin concentrations below 3 at. % exhibit good electrical conductivity on the order of 2×10^{-4} $(\Omega \cdot cm)^{-1}$. Owing to their high transparency and good electrical conductivity, Sn-doped ZnO thin films are promising candidates for various optoelectronic applications, particularly in dye-sensitized photovoltaic solar cells.

Keywords: Zinc oxide, Thin films, Tin doping ratio, Solar spray pyrolysis, Solar heater.

DOI: 10.21272/jnep.18(2).02038 PACS numbers: 07.20.Hy, 73.50.Pz

1. INTRODUCTION

Zinc oxide (ZnO) has attracted significant attention in recent years as a transparent conducting oxide (TCO) due to its excellent electronic and optical properties [1]. ZnO is an *n*-type semiconductor belonging to the II-VI group [2], with a large exciton binding energy of 60 meV [3] and a wide direct band gap of 3.34 eV [4, 5]. Pure ZnO thin films, however, exhibit relatively low optical transmittance and electrical conductivity due to their low carrier density. To enhance these physical properties, ZnO is commonly doped with various elements such as Sn, Al, F, Ge, Ti, Bi, and Cu [6]. TCO thin films have been widely applied in a variety of devices, including solar cells [5], UV photodetectors and piezoelectric transducers [4], as well as gas sensors [6]. Several deposition techniques have been employed to prepare ZnO thin films, including successive ionic layer adsorption [1], chemical methods [7], pulsed laser deposition [8], and spray pyrolysis [2].

The aim of this study is to investigate the effect of tin incorporation on ZnO thin films as transparent conducting oxides for solar cell applications. ZnO films were prepared using the spray pyrolysis technique combined with solar heating, employing a solar furnace – a safe and economical method. The solar furnace, based on a parabolic dish, consists of a mirror layer (ITO glass) with a parabolic reflector and a substrate holder positioned at its focal point. Solar energy is concentrated by the reflector to heat a glass substrate fixed on the holder. Thin films were deposited by spray pyrolysis onto glass substrates maintained at 400 ± 15 °C, with tin doping concentrations of 0, 1, 3, 5, and 7 at.%.

In this work, the effect of tin (Sn) doping on the properties of ZnO thin films prepared by the solar spray pyrolysis technique was investigated. The structural, optical, and electrical properties of all films were examined to establish correlations with the doping concentration.

2. EXPERIMENTS

The sputtering solution was prepared using zinc chloride ($ZnCl_2$) (0.1 M) as a precursor in 100 ml of bi-distilled water. After stirring at 60 °C, an amount of Tin (II) chloride dehydrate ($SnCl_2$. $2H_2O$) with different ratio was dissolved into the solution (0, 1, 3, 5 and 7 at. %). The solution mixture was stirred for 1 hour at RT and heated to yield a clear solution, in these setup drops of HCl can be added as a stabilizer with heating. After that, the different prepared Sn-ratio solutions were sprayed on 450 ± 15 °C preheated glass substrates by solar spray pneumatic method using solar furnace (see Figure 1a and 1b) for 10 minutes of deposition time and

* Correspondence e-mail: benramache.said@gmail.com

Cite this article as: A. Nid et al., *J. Nano- Electron. Phys.* 18 No 2, 02038 (2026) https://doi.org/10.21272/jnep.18(2).02038

1 ml/min solution flow rate.

The prepared Sn-doped ZnO thin films were characterized at room temperature using an X-ray diffractometer (Bruker AXS, type 8D) with CuKα radiation ($\lambda = 0.15406$ nm) over a 2θ range of 20-70°. Optical transmittance spectra were recorded in the wavelength range of 300-900 nm using a UV-visible spectrophotometer (Lambda 35). Electrical properties were measured using the four-point probe method with a Keithley 2400-LV Source Meter.

3. RESULTS AND DISCUSSION

The effects of Sn doping on the crystal structure and preferred orientations of ZnO thin films were investigated using X-ray diffraction (XRD). Figure 2 presents the XRD patterns of the prepared Sn-doped ZnO films deposited onto glass substrates with various Sn doping concentrations. The diffraction peaks are well indexed to the hexagonal wurtzite structure of ZnO, in agreement with JCPDS Card No. 36–1451 [9]. The three main diffraction peaks were observed at approximately $2\theta \approx 31°$, 34°, and 36°, corresponding to the (100), (002), and (101) crystallographic planes, respectively.

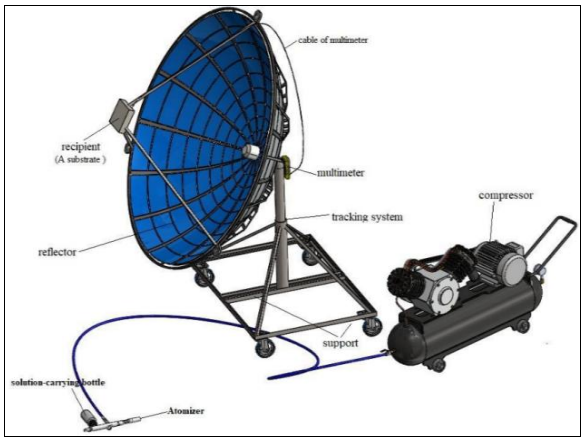

Fig. 1 – Complete assembly of the experimental setup (Designed by Solid Works)

The second result, no extra peaks corresponding to other phases such as tin oxide or other tin compounds were detected, this shows the good incorporation of Sn atoms in the ZnO matrix and therefore the success of the doping. Furthermore, the obtained ZnO:Sn thin films exhibit highest intensity for (002) plane which shows that they are preferentially oriented along *c*-axis.

In order to get further structural informations, several structural parameters of Sn-doped ZnO thin films were calculated, such as the interplanar spacing d_{hkl}, crystallite size D, lattice strain ε, and dislocation density δ. The interplanar spacing d_{hkl} is calculated by Bragg's law [10]:

$$2d_{hkl}\sin\theta = n\lambda \qquad (1)$$

where θ is the Bragg diffraction angle of peak in degree, n is the order of diffraction taken equal unity (first order), and λ is the wavelength of the incident radiation ($\lambda = 1.5406$ Å).

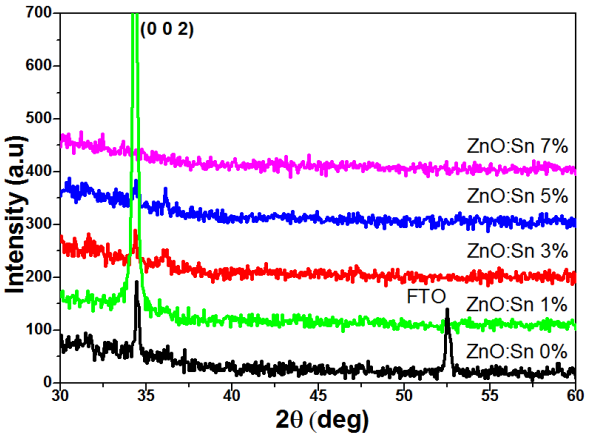

Fig. 2 – X-Ray diffraction spectra of ZnO:Sn thin films elaborated at 400 °C.

The crystallite size D of the films was calculated for (002) plane using Scherrer's formula [7-8]:

$$D_{hkl} = \frac{k\lambda}{\beta\cos\theta} \qquad (2)$$

where λ is the X-ray wavelength and β is the full width at half maximum (FWHM) corresponding to Bragg's diffraction angle θ. The dislocation density δ, which is defined as the dislocation lines per unit volume of crystal, was calculated using the following formula [11]:

$$\delta_{hkl} = \frac{1}{D_{hkl}} \qquad (3)$$

Table 1 summarizes the variations of the structural parameters of the prepared Sn-doped ZnO thin films with different tin doping concentrations. Examination of the results indicates that the degree of preferential orientation decreases with increasing doping level. Furthermore, the crystallite sizes along the [002] crystallographic plane were observed to decrease with increasing Sn content, suggesting that Sn doping reduces the crystallinity of ZnO thin films, as previously reported in several studies [12]. In addition, a slight shift of the (002) diffraction peak toward lower angles compared to pure ZnO is observed upon $SnCl_2$ incorporation. This shift indicates an increase in the interplanar spacing, which is consistent with the substitution of larger Sn^{4+} ions for Zn^{2+} ions. It is known that Sn ions can exist in different oxidation states, such as Sn^{2+} and Sn^{4+}, with ionic radii of 0.62 Å and 0.69 Å, respectively [13].

To investigate the optical properties of the deposited Sn-doped ZnO thin films as a function of Sn doping concentration, the optical transmittance spectra of the films were measured and are presented in Figure 3. The results show that the optical transparency of the films increases with Sn doping. The average transmittance rises from 73 % for the undoped ZnO film to 90 % for the film doped with 3 at. % Sn, corresponding to an increase of approximately 17%. This enhancement in transparency can be attributed to a reduction in surface roughness induced by Sn incorporation [14]. Consequently, ZnO films doped with 3 at. % Sn are well suited for applications as transparent conductive layers in various optoelectronic devices, including photovoltaic cells.

Table 1 – Structural parameters deduced from the (002) peak of Sn-doped ZnO thin films with various Sn doping ratios

Sn doping ratio (at. %)	Diffraction angle 2θ (°)	FWHM β (°)	Interplanar spacing d_{hkl} (Å)	Crystallite size D (nm)	Lattice strain ε (%)	Dislocation density $\sigma \times 10^{15}$ (lines/m^2)
0	34.473	0.197	2.602	42.265	0.277	0.517
1	34.360	0.300	2.608	27.717	0.423	1.231
3	34.320	0.295	2.613	28.165	0.417	1.189
5	34.180	0.787	2.623	10.558	1.117	8.734

For higher Sn concentrations (greater than 3 at. %), the transmittance decreases, likely due to increased photon scattering caused by crystal defects generated during doping [15].

The value of the optical band gap energy of all samples was calculated; we used the Tauc relation [16]. This was done by plotting $(\alpha h\upsilon)^2$ as a function of the photon energy $h\upsilon$ according to equations (4 and 5) [17]:

$$A = \alpha t = -LnT \tag{4}$$

$$(\alpha h\upsilon)^n = B(h\upsilon - E_g) \tag{5}$$

where A is the absorbance, d is the film thickness, T is the transmittance spectra of thin films α is the absorption coefficient values, B is a constant, $h\upsilon$ is the photon energy and E_g is the band gap energy. We take $n = 2$ for direct band gap semiconductors.

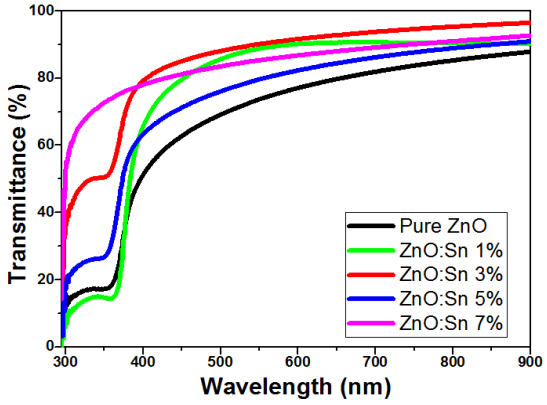

Fig. 3 – Spectral transmittance curves of ZnO:Sn thin films with various Sn ratios

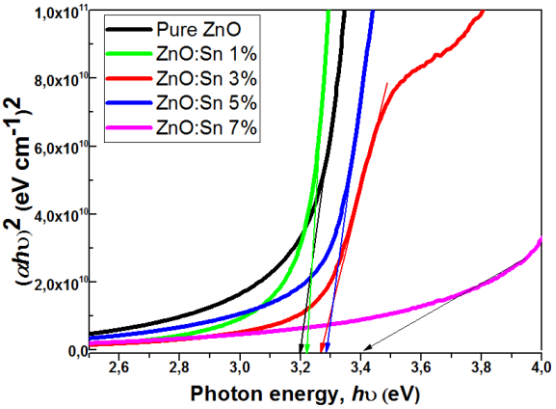

Fig. 4 – $(\alpha h\upsilon)^2$ variation versus $h\upsilon$ of each ZnO:Sn thin film with different Sn ratios

As shown in Figure 4, the optical band gap increases from 3.23 eV for the undoped ZnO films to 3.34 eV for ZnO films doped with 7 at. % Sn. This widening of the band gap can be attributed to the Burstein-Moss effect [18]. Additionally, doping introduces degenerate energy levels, which raise the Fermi level above the conduction band edge, further contributing to the band gap increase [5, 18]. To assess the degree of disorder in the thin films, the Urbach energy (E_u) was calculated using the following equation [16, 17]:

$$\alpha = \alpha_0 \exp\left(\frac{h\upsilon}{E_u}\right) \tag{6}$$

where: α_0 is a constant and E_u is the Urbach Energy, by plotting $Ln\alpha$ in terms of $h\upsilon$, we can ascertain the value of E_g as the reciprocal of the linear tangent that intersects the photon energy at $x = 0$ as shown in Figure 4. Figure 5 shows $Ln\alpha$ variation versus photon energy $h\upsilon$ for films. E_u values were calculated from reciprocal slopes of the straight lines.

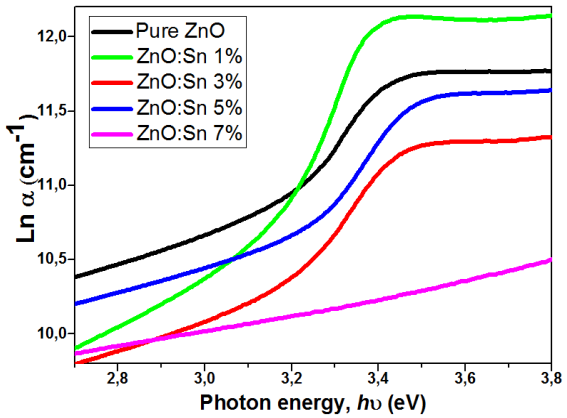

Fig. 5 – $Ln\alpha$ variation versus $h\upsilon$ of each ZnO:Sn thin film with different Sn ratios

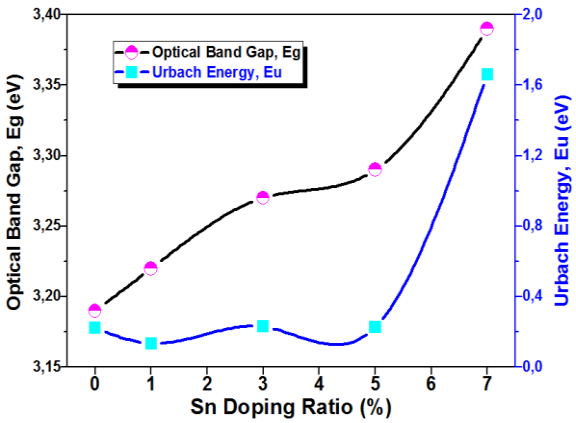

Fig. 6 – Variation of optical energy and urbach energy of ZnO:Sn films with different Sn doping ratios

Figure 6 shows the variation of the optical band gap and Urbach energy as a function of Sn doping. The increase in Urbach energy, which reflects the degree of disorder, with Sn incorporation is likely due to the deterioration of the structural quality of the films [19]. These results are consistent with the observations from the XRD analysis.

The four-point probes method was adopted to determine the electrical conductivity σ of Sn-doped ZnO films; the measurement was based on the sheet resistance R_{sh}. It's obtained by the following expression [20]:

$$R_{sh} = \frac{\pi}{Ln2}\frac{V}{I} \tag{7}$$

$$\sigma = \frac{1}{\rho} = \frac{1}{tR_{sh}} \tag{8}$$

where ρ is the electrical resistivity, t is the film thickness, I is the applied current (0.5×10^{-6} A) and V is the measurement voltage.

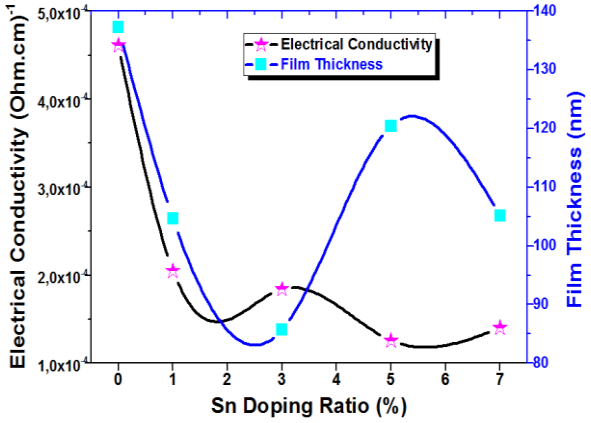

Figure 7 – Electrical conductivity σ vs. film thickness of ZnO:Sn films with different Sn doping ratios

Figure 7 shows the electrical conductivity and film thickness of Sn-doped ZnO films plotted as function of different Sn doping ratio. As can see from this plot, the electrical conductivity decreased to minimum value 1.26×10^{-4} $(\Omega{\cdot}\text{cm})^{-1}$ for sprayed with 5 at. % of tin, while the minimum obtained thickness was 86 nm for 3 at. % of Sn.

Despite the decreasing of electrical conductivity, it remains good values of the order of 2×10^{-4} $(\Omega{\cdot}\text{cm})^{-1}$ especially for doped ZnO films with 1 and 3 at. % of Sn, which makes them suitable for photovoltaic applications [5]. It is worth noting that the electrical conductivity (σ) of the elaborated Sn-ZnO films haven-type character.

4. CONCLUSION

In this work, Sn-doped ZnO thin films were successfully deposited onto glass substrates using the solar spray pyrolysis method at approximately 400 °C, employing a solar furnace as the heat source. The effect of tin incorporation (0–7 at. %) into the ZnO lattice was investigated through the analysis of the structural, optical, and electrical properties of the prepared films. X-ray diffraction (XRD) patterns revealed that the Sn-doped ZnO thin films possess a hexagonal wurtzite structure with a preferred orientation along the (002) plane. The calculated crystallite sizes indicated that the doped films exhibit smaller crystallite sizes compared with the undoped film. UV-visible spectroscopy showed that all films have high optical transparency, with an average transmittance of about 73 % for the undoped film, increasing to approximately 86 % after doping. The highest optical band gap value (3.34 eV) was obtained for the film doped with 7 at. % Sn. Electrical measurements revealed a high electrical conductivity on the order of $2{\cdot}10^{-4}$ $(\Omega{\cdot}\text{cm})^{-1}$ for the films doped with 1 and 3 at. % Sn. Based on these results, the prepared Sn-doped ZnO thin films can be considered promising candidates for optoelectronic applications, particularly in photovoltaic solar cells.

ACKNOWLEDGEMENTS

The authors would like to acknowledge Professor Boubaker Benhaoua for his support and assistance.

REFERENCES

1. R. Fan, F. Lu, K. Li, *J. Lumin.* **192**, 410 (2017) https://doi.org/10.1016/j.jlumin.2017.07.003.
2. H. Aydin, H.M. El-Nasser, C. Aydin, A.A. Al-Ghamdi, F. Yakuphanoglu, *Appl. Surf. Sci.* **350**, 109 (2015) https://doi.org/10.1016/j.apsusc.2015.02.189.
3. A. Ouhaibi, M. Ghamnia, M.A. Dahamni, V. Heresanu, C. Fauquet, D. Tonneau, *J. Sci. Adv. Mater. Dev.* **3**, 29 (2018) https://doi.org/10.1016/j.jsamd.2018.01.004.
4. A. Janotti, C.G. Van de Walle, *Rep. Prog. Phys.* **72**, 126501 (2009) https://doi.org/10.1088/0034-4885/72/12/126501.
5. F.Z. Bedia, A. Bedia, N. Maloufi, M. Aillerie, F. Genty, B. Benyoucef, *J. Alloy Compd.* **616**, 312 (2014) https://doi.org/10.1016/j.jallcom.2014.07.086.
6. H. Liu, V. Avrutin, N. Izyumskaya, Ü. Özgür, H. Morkoç, *Superlattice. Microstruct.* **48**, 458 (2010) https://doi.org/10.1016/j.spmi.2010.08.011.
7. A. Diha, L. Fellah, S. Benramache, O. Belahssen, *Defect Diff. Forum* **406**, 285 (2021) https://doi.org/10.4028/www.scientific.net/DDF.406.285
8. D. Souad, S. Benramache, A. Ammari, A. Gahtar, *Iran. J. Phys. Res.* **22**, 185 (2022) https://doi.org/10.47176/ijpr.22.3.01590.
9. T. Saoud, S. Benramache, A. Diha, *Chemistry-Didactics-Ecology-Metrology* **28**, 171 (2023) https://doi.org/10.2478/cdem-2023-0010.
10. J. Wang, P. Yang, X. Wei, Z. Zhou, *Nanoscale Res. Lett.* **10**, 119 (2015) https://doi.org/10.1186/s11671-015-0807-5.
11. M.N. Amroun, K. Salim, A.H. Kacha, M. Khadraoui, *Int. J. Thin. Film. Sci. Tech.* **9**, 103 (2020) https://doi.org/10.18576/ijtfst/090203.
12. M. Vasanthi, K. Ravichandran, N. Jabena Begum, G. Muruganantham, S. Snega, A. Panneerselvam, P. Kavitha, *Superlattice. Microstruct.* **55**, 180 (2013) https://doi.org/10.1016/j.spmi.2012.12.011.
13. A. Palacios-Padros, M. Altomare, K. Lee, I. Díez-P´erez, F. Sanz, P. Schmuki, *ChemElectroChem* **1**, 1133 (2014) https://doi.org/10.1002/celc.201402002.
14. K. Salim, M. Medles, A. Nakrela, R. Miloua, A. Bouzidi, R.

Desfeux, *Optik* **210**, 164 (2020) https://doi.org/10.1016/j.ijleo.2020.164504.
15. S.S. Shinde, A.P. Korade, C.H. Bhosale, K.Y. Rajpure, *J. Alloy. Compd.* **551**, 688 (2013) https://doi.org/10.1016/j.jallcom.2012.11.057.
16. W. Daranfed, M.S. Aida, A. Hafdallah, H. Lekiket, *Thin Solid Films* **518**, 1082 (2009) https://doi.org/10.1016/j.tsf.2009.03.227.
17. A. Sbaihi, S. Benramache, C. Benbrika, *J. Nano- Electron. Phys.* **16** No 1, 01022 (2024) https://doi.org/10.21272/jnep.16(1).01022.
18. N. Rajeswari Yogamalar, A. Chandra Bose, *Appl. Phys. A* **103**, 33 (2013) https://doi.org/10.1007/s00339-011-6304-5.
19. C.Y. Tsay, H.C. Cheng, Y.T. Tung, W.H. Tuan, L. Chung Kwei, *Thin Solid Films* **517**, 1032 (2008) https://doi.org/10.1016/j.tsf.2008.06.030.
20. B. Maaoui, Y. Aoun, S. Benramache, *Nanosistemi, Nanomateriali, Nanotehnologii* **19**, 167 (2021) https://doi.org/10.15407/nnn.19.01.167.

Властивості тонких плівок ZnO, легованих Sn, створених шляхом піролізу сонячного розпилення для фотоелектричних застосувань

Abdelbaki Nid[1,2,3], Lilia Zighed[1,2,3], Yacine Aoun[4], Said Benramache[5]

[1] *Mechanical Department, Faculty of Technology, University of Skikda, Skikda 21000, Algeria*
[2] *LGMM Laboratory, Faculty of Technology, University of Skikda, Skikda 21000, Algeria*
[3] *LGCES Laboratory, Faculty of Technology, University of Skikda, Skikda 21000, Algeria*
[4] *Mechanical Department, Faculty of Technology, University of El-Oued, El-Oued 39000, Algeria*
[5] *Laboratoire des Matériaux, des Énergies et de l'Environnement, University of Biskra 07000, Algeria*

У роботі тонкі плівки чистого оксиду цинку та легованого оловом ZnO(ZnO:Sn) були отримані на скляних підкладках методом піролізу. Структурні, оптичні та електричні властивості плівок ZnO, легованих оловом, досліджувалися при різних співвідношеннях легування оловом (0, 1, 3, 5 і 7 ат. %). Результати XRD показують, що всі плівки мають полікристалічні властивості. гексагональна вюрцитна структура зі сприятливою орієнтацією вздовж площини (002). Спектроскопічні вимірювання УФ-видимості показують, що всі плівки мають гарне оптичне пропускання з високим коефіцієнтом пропускання близько 90 % для легованої плівки з 3 ат. % Sn. Величина оптичної щілини зростає в діапазоні від 3,23 до 3,34 еВ зі збільшенням вмісту олова. Установлено, що леговані шари з вмістом олова менше 3 ат. % мають хорошу електропровідність порядку 2×10^{-4} (Ом·см)$^{-1}$. Завдяки високій прозорості та електропровідності ZnO, легованого Sn, його можна використовувати в різних оптоелектронних пристроях, таких як сенсибілізовані барвником фотоелектричні сонячні елементи.

Ключові слова: Оксид цинку, Тонкі плівки, Коефіцієнт легування оловом, Сонячний піроліз; Сонячний обігрівач.